HHS Public Access

Author manuscript

J Thromb Haemost. Author manuscript; available in PMC 2024 December 01.

Published in final edited form as:

J Thromb Haemost. 2023 December ; 21(12): 3619–3632. doi:10.1016/j.jtha.2023.08.026.

PACSIN2 regulates platelet integrin β1 hemostatic function

Ratnashree Biswas[1,2,*], **Emily K. Boyd**[1,2,3,*], **Nathan Eaton**[1,2,3], **Agata Steenackers**[1,2], **Marie L. Schulte**[1], **Friedrich Reusswig**[1,2], **Hongyin Yu**[1,3], **Caleb Drew**[1,2], **Walter H. A. Kahr**[4,5], **Qizhen Shi**[1,3,6,7], **Markus Plomann**[8], **Karin M. Hoffmeister**[1,2,9], **Hervé Falet**[1,2,3]

[1]Versiti Blood Research Institute, Milwaukee, Wisconsin, USA

[2]Translational Glycomics Center, Milwaukee, Wisconsin, USA

[3]Department of Cell Biology, Neurobiology, and Anatomy, Medical College of Wisconsin, Milwaukee, Wisconsin, USA

[4]Program in Cell Biology, The Hospital for Sick Children, Toronto, Ontario, Canada

[5]Departments of Paediatrics and Biochemistry, University of Toronto, Toronto, Ontario, Canada

[6]Department of Pediatrics, Medical College of Wisconsin, Milwaukee, Wisconsin, USA

[7]Children's Research Institute, Children's Wisconsin, Milwaukee, Wisconsin, USA

[8]Center for Biochemistry, Medical Faculty, University of Cologne, Cologne, Germany

[9]Departments of Biochemistry and Medicine, Medical College of Wisconsin, Milwaukee, Wisconsin, USA

Abstract

Background: Upon vessel injury, platelets adhere to exposed matrix constituents via specific membrane receptors, including the von Willebrand factor receptor GPIb-IX-V complex and integrins β1 and β3. In platelets, the F-BAR protein PACSIN2 associates with the cytoskeletal and scaffolding protein filamin A (FlnA), linking GPIbα and integrins to the cytoskeleton.

Objectives: Here we investigated the role of PACSIN2 in platelet function.

Methods: Platelet parameters were evaluated in mice lacking PACSIN2 and platelet integrin β1.

Correspondance: Hervé Falet, Versiti Blood Research Institute, 8727 W Watertown Plank Rd, Milwaukee, WI 53226, USA. hfalet@versiti.org.

*Contributed equally.

Author contributions

RB and EKB performed experiments, collected, analyzed, and interpreted data, and wrote and revised the manuscript. NE, AS, MLS, FR, HY, and CD, performed experiments, collected, analyzed, and interpreted data, and revised the manuscript. WHAK, QS, and KMH analyzed and interpreted data and revised the manuscript. MP generated the *Pacsin2*$^{-/-}$ mice and revised the manuscript. HF conceived and designed the study, performed experiments, collected, analyzed, and interpreted data, and wrote and revised the manuscript. All authors contributed to the article and approved the submitted version.

Conflict of interest

The authors declare that the research was conducted in the absence of any commercial or financial relationships that could be construed as a potential conflict of interest.

Results: *Pacsin2*$^{-/-}$ mice displayed mild thrombocytopenia, prolonged bleeding time, and delayed thrombus formation in a ferric chloride-mediated carotid artery injury model, which was normalized by injection of control platelets. *Pacsin2*$^{-/-}$ platelets formed unstable thrombi that embolized abruptly in a laser-induced cremaster muscle injury model. *Pacsin2*$^{-/-}$ platelets had hyperactive integrin β1, as evidenced by increased spreading onto surfaces coated with the collagen receptor α2β1-specific peptide GFOGER and increased binding of the antibody 9EG7 directed against active integrin β1. By contrast, *Pacsin2*$^{-/-}$ platelets had normal integrin αIIbβ3 function and expressed P-selectin normally following stimulation through the collagen receptor GPVI or with thrombin. Deletion of platelet integrin β1 in *Pacsin2*$^{-/-}$ mice normalized platelet count, hemostasis, and thrombus formation. A PACSIN2 peptide mimicking the FlnA binding site mediated the pull-down of a FlnA rod 2 construct by integrin β7, a model for integrin β-subunits.

Conclusions: *Pacsin2*$^{-/-}$ mice displayed severe thrombus formation defects due to hyperactive platelet integrin β1. The data suggest that PACSIN2 binding to FlnA negatively regulates platelet integrin β1 hemostatic function.

Keywords

platelets; PACSIN2; filamin A; integrin β1

1. Introduction

Blood platelets are anucleate, discoid cells that regulate hemostasis. Upon blood vessel injury, platelets adhere to the exposed extracellular matrix, resulting in platelet shape change, activation, and aggregation to form a hemostatic plug [1]. Platelet adhesion requires the contribution of a wide variety of platelet receptors such as the von Willebrand factor (VWF) receptor GPIb-IX-V complex, the collagen receptor GPVI, and integrins [2]. Platelets contain five integrins of the β1 and β3 families. Integrins α2β1, α5β1, and α6ββ1 mediate adhesion to the extracellular matrix proteins collagen, fibronectin, and laminin, respectively, while integrins αIIbβ3 and αVβ3 bind to plasma fibrinogen and vitronectin, respectively [3]. At low shear stress, platelets adhere to exposed collagen through integrin α2β1 and activate through GPVI [4]. At higher shear stress, plasma VWF binds to exposed collagen, thereby becoming an essential adhesive protein for both adhesion and aggregation [2]. The GPIb-IX-V complex and integrin αIIbβ3 bind VWF in a coordinated and synergistic manner, each contributing unique biochemical properties to support thrombus formation.

The Fes/CIP4-homology Bin-Amphiphysin-Rvs (F-BAR) protein PACSIN2 remodels membranes and the actin cytoskeleton to regulate receptor internalization, caveolae biogenesis, endosomal trafficking, cell adhesion, spreading, and migration [5]. PACSIN2 contains a flexible N-terminal F-BAR domain which tubulates membranes, three central NPF motifs which are docking sites for endocytic Eps15 homology domain proteins, and a C-terminal Src homology 3 domain which interacts with endocytic and actin regulatory proteins such as dynamin 2 and N-WASP. PACSIN2 is one of the most abundant and conserved platelet BAR proteins [6–8], and exome-chip and genome-wide association studies have associated single nucleotide polymorphisms (SNPs) in *PACSIN2* with platelet count (PLT), mean platelet volume (MPV), platelet distribution width (PDW), and platelet-

to-lymphocyte ratio (PLR) in humans [9–13]. For MPV, *P*-values are as low as 4 x 10^{-216} [14], well below the commonly accepted 5 x 10^{-8} significance threshold [15].

The cytoskeletal and scaffolding protein filamin A (FlnA) participates in the anchoring of platelet receptors, notably GPIbα and integrin β-subunits, to the actin cytoskeleton [16]. FlnA is composed of an N-terminal calponin-homology actin-binding domain and 24 immunoglobulin-like repeats forming an elongated rod 1 (repeats 1-15), a compact rod 2 (repeats 16-23), and a C-terminal dimerization domain (repeat 24) [17]. The GPIb-IX-V complex subunit GPIbα binds to repeat 17 [18], while integrin β-subunits bind to repeat 21 [19, 20]. The FlnA-GPIbα interaction is constitutive and plays a critical role in platelet production, morphology, and function, as evidenced by the macrothrombocytopenia of Bernard-Soulier Syndrome (BSS) patients with *GP1BA, GP1BB*, and *GP9* mutations and patients with *FLNA* mutations [21]. By contrast, the binding of integrin β-subunits to FlnA repeat 21 is masked by a β-strand in repeat 20, requiring conformational changes in FlnA [22, 23]. PACSIN2 over-expression in Xenopus XTC cells prevents the localization of integrin α5β1 to focal adhesions and FlnA to stress fibers, suggesting that PACSIN2 controls the population of activated integrins and cytoskeleton strength during cell movement [24].

We have previously shown that PACSIN2 binds FlnA in platelets and megakaryocytes (MKs), where it localizes with the initiating demarcation membrane system (DMS) [25]. The FlnA-PACSIN2 interaction requires FlnA repeat 20 and the tip of the PACSIN2 F-BAR domain. Here, we investigated the role of PACSIN2 in platelet hemostatic functions. *Pacsin2*$^{-/-}$ mice displayed severe thrombus formation defects due to hyperactive integrin β1 in platelets in the presence of mild thrombocytopenia.

2. Materials and methods

2.1. Mice

Pacsin2$^{-/-}$ mice were generated by Dr. Markus Plomann (University of Cologne, Germany) [26, 27]. *Itgb1*$^{fl/fl}$ mice and transgenic *Pf4-Cre* mice were obtained from the Jackson Laboratory (strains 4605 and 8535, respectively) and crossed to delete *Itgb1* in MKs and platelets [28]. Studies were performed on 8-12-week-old female and male mice backcrossed in the C57BL/6 background. Mice were treated according to the National Institutes of Health and Medical College of Wisconsin Institutional Animal Care and Use Committee Guidelines.

2.2. Complete blood count

Mice were anesthetized via intraperitoneal injection of ketamine/xylazine. Blood was collected from the retroorbital plexus using EDTA-coated capillary tubes. Complete blood counts were measured on a Sysmex XT-2000i automatic hematology analyzer [29, 30].

2.3. Platelet preparation and confocal microscopy

Blood was collected by retroorbital bleeding in 100 μL of acid-citrate-dextrose. Platelets were isolated by centrifugation and resuspended at 5 x 10^8 platelets/mL. Platelets were

seeded onto glass coverslips coated with 5% BSA (resting), fibrinogen or the collagen-related peptide GFOGER (O = hydroxyproline), specific for the collagen receptor α2β1 [31, 32], and incubated in 10 μg/mL collagen-related peptide $GCO(GPP)_{10}GCOG$ (CRP; Versiti Blood Research Institute Protein Chemistry Core Laboratory), specific for the collagen receptor GPVI [33], or 0.01 U/mL human thrombin (Roche) at 37°C for 30 min (spread) [29, 30]. Imaging was performed on an Olympus Confocal FV1000-MPE platform using a UPlanSApo 100x/1.40 oil objective and FluoView software. The surface area of individual platelets was measured using Imaris (Oxford Instruments) software. Quantification was performed blinded.

2.4. Platelet survival

Endogenous platelet survival was performed by retroorbitally injecting biotin-NHS (Calbiochem) into *Pacsin2*$^{+/+}$ and *Pacsin2*$^{-/-}$ mice. Exogenous platelet survival was performed by injection of *Pacsin2*$^{+/+}$ and *Pacsin2*$^{-/-}$ platelets fluorescently labeled with 5 μM CMFDA (Invitrogen) into control mice. Blood samples were collected immediately (<2 min) and up to 96 h after injection. Biotinylated platelets were stained with streptavidin-PE (Thermo Fisher Scientific). The percentage of PE- or CMFDA-positive platelets was quantified by flow cytometry [28].

2.5. Immunohistochemistry

Seven-μm mouse femur sections were prepared as described [30]. Sections were incubated with monoclonal rat-anti-GPIbα (Emfret Analytics) and polyclonal rabbit-anti-laminin (Sigma-Aldrich) followed by incubation with Alexa Fluor 488 and 568 secondary antibodies (Molecular Probes), respectively. Surfaces were created toward the greatest signal intensities of GPIbα-positive cells using thresholds for cell size and quantitatively analyzed using Imaris and Excel (Microsoft) software.

2.6. Transmission electron microscopy

Bone marrow cells were obtained by flushing mouse femurs with 2.5% glutaraldehyde in phosphate-buffered saline [25]. After overnight fixation, cells were postfixed with 2% osmium tetroxide in H_2O for 1 h and dehydrated in a graded acetone series before embedding in Epon-Araldite. Thin sections were cut and stained with uranyl acetate and lead citrate. Grids were examined with a JEOL JEM-1011 electron microscope at 80 kV. Images were captured with a side-mounted Advantage HR CCD camera (Advanced Microscopy Techniques).

2.7. Tail bleeding time

Bleeding time was defined as complete cessation of bleeding after snipping 2 mm of distal mouse tail and immediate immersion in 37°C isotonic saline [29, 30].

2.8. Ferric chloride-induced thrombosis

The right carotid artery was exposed, and a 1x2 mm filter paper soaked in freshly prepared 10% anhydrous $FeCl_3$ was placed on it for 3 min. After rinsing with saline, a Doppler probe was placed, and subsequent readings were recorded [30].

2.9. Laser-induced injury

Intravital imaging of platelet thrombus formation in male mouse cremaster arterioles was performed in the Versiti Blood Research Institute Thrombosis Core Laboratory [30]. Laser intensity and duration were adjusted to produce an injury visible in the brightfield image. The Ablate! laser ablation system (Intelligent Imaging Innovations) uses a 532 nm pulse laser (>60 μJ pulses at 200 Hz) to enable controlled vessel damage and initiation of thrombus formation. Injuries were created using between 1 and 5 pulses within a 20 s time window. The laser energy ranged from 60 to 75%. Fluorescence images were captured using a high-speed Orca Flash 4.0 camera (Hamamatsu). Data were collected for 3 min following vessel injury.

2.10. Ex vivo perfusion assay

Adhesion assays on type I collagen (Chrono-log) were performed in whole blood using the VenaFlux (Cellix) microfluidic perfusion platform an arterial shear rate of 1500 s^{-1} [30]. Images were brightness corrected and converted to a binary mask with software provided auto-thresholds. Binary Mask Particles were then analyzed to determine surface area and dwell time using Imaris software.

2.11. Flow cytometry

Surface expression of platelet receptors was detected by flow cytometry using fluorescently conjugated antibodies against GPIbα, GPIbβ, GPIX, GPV, GPVI, and integrins α2, α5 (Emfret Analytics), β1, β3, and αIIb (BD Biosciences) [30]. Platelets were activated with CRP or thrombin for 2 min at 37°C and stained for 30 min at room temperature with a FITC-labeled rat anti-mouse P-selectin antibody (BD Biosciences) or Oregon Green 488-labeled fibrinogen (Thermo Fisher Scientific) [34]. Integrin β1 activation was evaluated using rat antibody 9EG7 (BD Biosciences), specific for active mouse integrin β1 [35, 36]. Fluorescence was quantified using an Accuri C6 Flow Cytometer or a FACSymphony A5 Cell Analyzer (BD Biosciences) and analyzed using FlowJo software.

2.12. Platelet aggregation

Platelet aggregation was monitored for 5 min at 37°C by light transmission under stirring conditions using a Chrono-log Model 490-X aggregometer [30].

2.13. Native rotational thromboelastometry

Blood was collected by the inferior vena cava and anticoagulated in sodium citrate. Three hundred μL of citrated blood samples were gently mixed with 21 μL of 200 mM $CaCl_2$ in conventional ROTEM cup by pipetting up and down once. Samples were tested for 1 h using ROTEM delta (Instrumentation Laboratory) [37]. Parameters measured include whole blood clotting time, defined as the time it takes to reach 2 mm in amplitude; clot formation time, defined as the time it takes an amplitude of 2 mm to reach 20 mm; maximum clot firmness; α-angle; and amplitude at 10 min.

2.14. Clot retraction assay

Washed mouse platelets were resuspended in citrated human platelet-poor plasma ($4\alpha10^8$ platelets/mL). Coagulation was triggered by the addition of 0.5 U/mL thrombin. Clots were allowed to retract for 1 h. The extent of clot retraction was determined as the volume of serum extruded from the clot and expressed a percentage of the total reaction volume [38].

2.15. Pull-down assay

An integrin β7 peptide containing the FlnA repeat 21 binding site (residues 752-770; Biomatik) was conjugated to SulfoLink agarose resin (Thermo Fisher Scientific) and incubated with 500 nM His-FlnA repeats 16-23 or His-eGFP-FlnA repeat 21 for 1 hour at 4°C in 1% Nonidet P-40, 150 mM NaCl, and 50 mM Tris, pH 7.4 in the presence or absence of 5 μM of a PACSIN2 peptide mimicking the FlnA repeat 20 binding site (residues 171-189; Biomatik) [25, 39]. After washing, complexes were resolved by SDS-PAGE and immunoblot analysis.

2.16. Statistical analysis

Statistical analysis was performed using Prism 10 software (GraphPad), with $P < .05$ considered significant. Two independent means were compared using the unpaired Student's t-test. Normal distribution was confirmed using quantile-quantile (Q-Q) plots. Results are presented as mean ± SD. Time-to-event data were estimated using the Kaplan-Meier method.

3. Results

3.1. Mild thrombocytopenia in *Pacsin2*$^{-/-}$ mice

Hematological parameters were evaluated in *Pacsin2*$^{-/-}$ mice (Table 1). *Pacsin2*$^{-/-}$ mice developed mild thrombocytopenia with 899 ± 267 x 10^3 platelets/μL, compared to 1178 ± 135 x 10^3 platelets/μL in *Pacsin2*$^{+/+}$ mice (n = 12 in each group; $P = .0043$). While MPV appeared normal, PDW, which reflects variability in platelet size and is considered a marker of platelet function and activation, was slightly increased in *Pacsin2*$^{-/-}$ mice ($P = .0054$). All other blood parameters were comparable to controls, except for mean corpuscular volume (MCV) and mean corpuscular hemoglobin (MCH), which were decreased in *Pacsin2*$^{-/-}$ mice.

The surface area of peripheral blood *Pacsin2*$^{-/-}$ platelets was measured by confocal microscopy after β-tubulin staining of the microtubule coils (Figure 1A, B). *Pacsin2*$^{-/-}$ platelets had a surface area of 8.16 ± 0.26 μm^2 (n = 122), compared to 7.54 ± 0.14 μm^2 for *Pacsin2*$^{+/+}$ platelets (n = 239; $P = .0223$). Although slightly larger, *Pacsin2*$^{-/-}$ platelets appeared discoid, and their marginal band was not brighter than that of control platelets. Fibrinogen was observed in large puncta in *Pacsin2*$^{-/-}$ platelets (Figure 1A), indistinguishable from *Pacsin2*$^{+/+}$ platelets, consistent with normal αIIbγ3-mediated uptake from plasma and retention into α-granules.

Pacsin2$^{-/-}$ platelets had a half-life of 44.8 ± 2.8 h (n = 4), compared to 42.9 ± 1.2 h for *Pacsin2*$^{+/+}$ platelets (n = 5; $P = .2031$) when measured in situ (Figure 1C). Transfused

Pacsin2$^{-/-}$ platelets also circulated normally in control mice, with a half-life of 47.2 ± 1.8 h (n = 4), compared to 47.7 ± 1.2 h for *Pacsin2*$^{+/+}$ platelets (n = 3; $P = .7231$) (Figure 1D).

The expression levels of the major membrane glycoproteins, i.e., the GPIb-IX-V complex, GPVI, and integrins β1 and β3, on *Pacsin2*$^{-/-}$ platelets were indistinguishable from controls (Table 1). Immunoblot analysis confirmed that *Pacsin2*$^{-/-}$ platelets expressed GPIbα and integrins β1 and β3 normally (Figure 1E). No apparent change in molecular weight was observed, indicating comparable glycan decorations in both genotypes. *Pacsin2*$^{-/-}$ platelets expressed FlnA normally.

3.2. Impaired demarcation membrane system formation in *Pacsin2*$^{-/-}$ megakaryocytes

Megakaryopoiesis was investigated in *Pacsin2*$^{-/-}$ mice (Figure 1F, **top panel)**. *Pacsin2*$^{-/-}$ bone marrow sections had normal MK count, with 55.0 ± 11.1 MKs per mm^2 (n = 8), compared with 61.2 ± 12.6 MKs per mm^2 in *Pacsin2*$^{+/+}$ bone marrow sections (n = 7; $P = .3287$), as quantified by GPIbα immunofluorescence (Figure 1G).

The ultrastructure of bone marrow MKs was examined by transmission electron microscopy, focusing on the DMS, the highly organized intracellular membrane reservoir for future platelets (Figure 1F, **bottom panel)**. Compared to control *Pacsin2*$^{+/+}$ MKs, the DMS appeared less well-defined in *Pacsin2*$^{-/-}$ MKs. Notably, distinct platelet territories were not readily visualized.

3.3. Bleeding and vessel occlusion defects in *Pacsin2*$^{-/-}$ mice

The role of PACSIN2 in hemostasis was evaluated (Figure 2A). *Pacsin2*$^{-/-}$ mice had a median tail bleeding time of 437.5 s, compared to 287.5 s in controls (n = 12 in each group; log-rank $P = .0040$). In 25% of the *Pacsin2*$^{-/-}$ mice, bleeding continued for 10 min, our experimental endpoint.

We then assessed vessel occlusion in *Pacsin2*$^{-/-}$ mice under high shear flow by using the $FeCl_3$-induced carotid artery injury model, in which blood flow rate is measured until occlusion. *Pacsin2*$^{-/-}$ mice had a median time to occlusive thrombosis of 370.5 s (n = 16), compared to 180 s in control *Pacsin2*$^{+/+}$ mice (n = 15; log-rank $P = .0071$) (Figure 2B).

Because PACSIN2 deletion is global, hemostasis in *Pacsin2*$^{-/-}$ mice was evaluated in the presence of control platelets. Retroorbital injection of 80 x 10^8 *Pacsin2*$^{+/+}$ platelets into *Pacsin2*$^{-/-}$ mice before $FeCl_3$-induced carotid artery injury normalized the median time to occlusive thrombus formation, comparable to that of *Pacsin2*$^{+/+}$ mice (Figure 2C). The data indicate that the thrombus formation defects of *Pacsin2*$^{-/-}$ mice were intrinsic to platelets, and not to extrinsic factors such as plasma or vessel wall abnormalities.

3.4. Rapid embolization of *Pacsin2*$^{-/-}$ platelet thrombi

To investigate the vessel occlusion defects in closer detail, we performed a cremaster vessel laser-induced injury model and documented acute thrombus development, enabling us to follow the simultaneous evaluation of platelet accumulation and fibrin deposition in real-time. Control *Pacsin2*$^{+/+}$ platelets adhered to the vessel wall at the site of injury and formed a thrombus over time (Figure 2D,E; Supplemental Video 1). Platelet accumulation appeared

rapidly in *Pacsin2*$^{-/-}$ mice, but thrombi were unstable and embolized repeatedly at 15 s intervals (Supplemental Video 2). Fibrin deposition was unaffected (Figure 2D,F). The data demonstrate that PACSIN2 plays an essential role in thrombus formation in vivo.

The functionality of *Pacsin2*$^{-/-}$ platelets to adhere to type I collagen and form thrombi under arterial shear rates (1500 s^{-1}) was examined in whole blood using the VenaFlux microfluidics platform (Figure 2G). After 3 min, the mean fluorescence intensity measured for *Pacsin2*$^{-/-}$ platelets was 2.92% ± 2.24% (n = 11), compared with 14.48 ± 13.70% in *Pacsin2*$^{+/+}$ controls (n = 9; $P = .0127$) (Figure 2H). We analyzed the dwell time of individual platelets under the same experimental conditions (Figure 2I). After initial tethering, control *Pacsin2*$^{+/+}$ platelets dwelled for a median time of 99 s (n = 60). *Pacsin2*$^{-/-}$ platelets dwelled for a significantly longer median time of 191 s (n = 60; Log-rank $P = .0463$), indicating increased stability of the GPIbα-VWF interaction in *Pacsin2*$^{-/-}$ platelets under arterial shear rates.

3.5. Normal activation and aggregation of *Pacsin2*$^{-/-}$ platelets in vitro

The significance of PACSIN2 expression in platelet hemostatic function was further examined in vitro. Platelets isolated from *Pacsin2*$^{+/+}$ and *Pacsin2*$^{-/-}$ mice were treated with the GPVI agonist CRP (Figure 3A,B) or the protease-activated receptor (PAR) agonist thrombin (Figure 3C,D) and analyzed by flow cytometry for CD62P (P-selectin) expression, as a marker for α-granule secretion (Figure 3A,C), or fluorescently labeled fibrinogen binding, as a marker of integrin αIIbγ3 activation (Figure 3B,D). CRP and thrombin induced comparable concentration-dependent increases of CD62P expression and fibrinogen binding in *Pacsin2*$^{+/+}$ and *Pacsin2*$^{-/-}$ platelets, reaching >80% of CD62P-expressing and fibrinogen-binding platelets with 10 μg/mL CRP or 0.1 U/mL thrombin.

Platelet aggregation to collagen was further assessed by light transmission under stirring conditions. *Pacsin2*$^{-/-}$ platelets aggregated normally in response to collagen concentrations of 5 μg/mL (Figure 3E) and 10 μg/mL (Figure 3F). The data indicate that *Pacsin2*$^{-/-}$ platelets display normal hemostatic function in vitro, i.e., α-granule secretion, integrin αIIbγ3 activation, and aggregation when stimulated with collagen, CRP, or thrombin.

3.6. Clot formation and retraction in *Pacsin2*$^{-/-}$ mice

The normal in vitro function measured using several agonists contrasts with the highly impaired in vivo platelet function. To further assess the viscoelastic properties of the blood clotting process, we performed the native ROTEM test on citrated and recalcified whole blood from *Pacsin2*$^{+/+}$ and *Pacsin2*$^{-/-}$ mice [37]. The median clotting time of *Pacsin2*$^{-/-}$ mice was 590.5 s, compared to 711.5 s in control *Pacsin2*$^{+/+}$ mice (n = 6 in each group; log-rank $P = .0046$), a 17% reduction (Figure 3G). All other parameters, i.e., clot formation time (Figure 3H), maximum clot firmness (Figure 3I), α-angle (Figure 3J), and amplitude at 10 min (Figure 3K), were comparable to controls.

Following inside-out αIIbβ3 integrin activation, fibrinogen binding triggers outside-in signaling, thereby driving clot firmness and retraction [40]. To evaluate the role of PACSIN2 in clot retraction, platelets isolated from *Pacsin2*$^{+/+}$ and *Pacsin2*$^{-/-}$ mice were resuspended in recalcified citrated human platelet-poor plasma, and coagulation was initiated by the

addition of 0.5 U/mL thrombin (Figure 3L) [38]. Clot retraction extruded similar serum volumes in the presence of *Pacsin2*$^{+/+}$ and *Pacsin2*$^{-/-}$ platelets. The data indicate that blood clotting in *Pacsin2*$^{-/-}$ mice was initially accelerated but normalized over time.

3.7. Increased integrin β1 activation in *Pacsin2*$^{-/-}$ platelets

We next investigated platelet spreading onto surfaces coated with fibrinogen, specific for the integrin αIIbβ3, or the collagen-related peptide GFOGER, specific for the integrin α2β1 (Figure 4A–C) [31, 32]. While *Pacsin2*$^{-/-}$ platelets spread normally onto surfaces coated with fibrinogen (Figure 4B), their spreading was increased onto surfaces coated with GFOGER (Figure 4C).

Because PACSIN2 over-expression in Xenopus XTC cells prevents the localization of integrin α5β1 to focal adhesions and FlnA to stress fibers [24], we measured the activation of integrin β1 in *Pacsin2*$^{-/-}$ platelets, using rat antibody 9EG7 directed against active mouse integrin β1 (Figure 4D) [35, 36]. Binding of 9EG7 to resting *Pacsin2*$^{-/-}$ platelets was increased two-fold, compared to *Pacsin2*$^{+/+}$ platelets (n = 5 in each group; $P = .0057$). By contrast, total surface integrin β1 expression was unaffected by PACSIN2 deletion (Table 1 and Figure 4E). The data indicate that PACSIN2 negatively regulates integrin β1 activation in resting platelets and upon activation.

3.8. PACSIN2 mediates integrin binding to FlnA rod 2

In full-length FlnA, a β-strand in incompletely folded repeat 20 masks the integrin binding site on repeat 21 [22, 23]. Because PACSIN2 binds to FlnA repeat 20 [25], we hypothesized that PACSIN2 may affect FlnA binding to integrin β-subunits. Using integrin β7 as a model [19], a peptide containing the FlnA repeat 21 binding site (residues 752-770) was conjugated to SulfoLink agarose resin and incubated with His-tagged FlnA repeats 16-23 (rod 2) in the presence or absence of a PACSIN2 peptide mimicking the FlnA repeat 20 binding site (residues 171-189) [25]. Integrin β7 pulled down FlnA repeats 16-23 in the presence, but not in the absence of the PACSIN2 peptide (Figure 4F). As control, integrin β7 pulled down FlnA repeat 21 independently of the PACSIN2 peptide. The data suggest that PACSIN2 binding to FlnA repeat 20 unmasks the integrin β-subunit binding site on FlnA repeat 21 (Figure 4G, **top panel**).

3.9. Normalization of platelet parameters in *Pacsin2*$^{-/-}$ mice lacking platelet integrin β1

To determine the contribution of integrin β1 hyperactivation to the hemostatic defects of *Pacsin2*$^{-/-}$ platelets in vivo, *Pacsin2*$^{-/-}$ mice were bred with *Itgb1*$^{fl/fl}$ *Pf4-Cre* (*Itgb1*$^{Plt-/-}$) mice lacking integrin β1 in platelets and MKs. Hematological parameters were evaluated in *Itgb1*$^{Plt-/-}$ *Pacsin2*$^{+/+}$ and *Itgb1*$^{Plt-/-}$ *Pacsin2*$^{-/-}$ mice (Table 2). While deletion of platelet integrin β1 did not affect platelet parameters in *Itgb1*$^{Plt-/-}$ *Pacsin2*$^{+/+}$ mice [28, 41–43], it normalized the mild thrombocytopenia and increased PDW in *Itgb1*$^{Plt-/-}$ *Pacsin2*$^{-/-}$ mice. The decreased MCV and MCH were unaffected by integrin β1 deletion in platelets, and other blood parameters were comparable to controls, pointing to the specificity of the normalized phenotype to the platelet and MK lineage.

Itgb1$^{Plt-/-}$ *Pacsin2*$^{-/-}$ platelets expressed normal levels of GPIb-IX-V, GPVI, and integrin β3 on their surface (Table 2). As expected, *Itgb1*$^{Plt-/-}$ *Pacsin2*$^{+/+}$ and *Itgb1*$^{Plt-/-}$ *Pacsin2*$^{-/-}$ platelets lacked integrins β1, α2, and α5. Immunoblot analysis confirmed that *Itgb1*$^{Plt-/-}$ *Pacsin2*$^{+/+}$ and *Itgb1*$^{Plt-/-}$ *Pacsin2*$^{-/-}$ platelets lacked integrin β1 but expressed GPIbα, integrin β3, and FlnA normally (Figure 1E).

3.10. Normalization of hemostatic function in *Pacsin2*$^{-/-}$ mice lacking platelet integrin β1

Itgb1$^{Plt-/-}$ *Pacsin2*$^{+/+}$ and *Itgb1*$^{Plt-/-}$ *Pacsin2*$^{-/-}$ mice had median tail bleeding times of 265 and 290 s, respectively (n= 12 in each group) (Figure 5A), comparable to controls (Figure 2A), indicating that platelet integrin β1 deletion normalized hemostasis in *Pacsin2*$^{-/-}$ mice.

We then assessed vessel occlusion in *Itgb1*$^{Plt-/-}$ *Pacsin2*$^{+/+}$ and *Itgb1*$^{Plt-/-}$ *Pacsin2*$^{-/-}$ mice using the $FeCl_3$-induced carotid artery injury model. *Itgb1*$^{Plt-/-}$ *Pacsin2*$^{-/-}$ mice had a median time to occlusive thrombosis of 226 s, compared to 187.5 s in *Itgb1*$^{Plt-/-}$ *Pacsin2*$^{+/+}$ mice (n = 12 in each group; log-rank $P = .9368$) (Figure 5B). Similarly, platelet integrin β1 deletion normalized platelet adhesion in the cremaster vessel laser-induced injury model (Figure 5C,D). Importantly, *Itgb1*$^{Plt-/-}$ *Pacsin2*$^{-/-}$ platelets formed stable thrombi that did not embolize. The data show that the thrombus formation defects and severe embolization of *Pacsin2*$^{-/-}$ mice were due to the hyperactivation of platelet integrin β1.

3.11. Clot formation and retraction in *Itgb1*$^{Plt-/-}$ *Pacsin2*$^{-/-}$ mice

We further performed the native ROTEM test on citrated and recalcified whole blood isolated from *Itgb1*$^{Plt-/-}$ *Pacsin2*$^{+/+}$ and *Itgb1*$^{Plt-/-}$ *Pacsin2*$^{-/-}$ mice (Figure 5E–I). All parameters measured were comparable to controls. Similarly, clot retraction extruded comparable serum volumes in the presence of *Itgb1*$^{Plt-/-}$ *Pacsin2*$^{+/+}$ and *Itgb1*$^{Plt-/-}$ *Pacsin2*$^{-/-}$ platelets (Figure 5J). The data suggest that accelerated clotting time of *Pacsin2*$^{-/-}$ mice was due to the hyperactivation of platelet integrin β1.

4. Discussion

We have previously shown that PACSIN2 binds FlnA in platelets and MKs, where it localizes with the initiating DMS and contributes to membrane tubulation during platelet production [25]. Here we demonstrated that *Pacsin2*$^{-/-}$ mice displayed mild thrombocytopenia with increased PDW, indicative of platelet activation, and slightly enlarged platelets, but indistinguishable platelet survival and glycoprotein expression from controls. MCV and MCH were also decreased in *Pacsin2*$^{-/-}$ mice, indicating microcytosis. While bone marrow MK numbers were normal, the DMS in freshly isolated *Pacsin2*$^{-/-}$ MKs appeared less well-defined than in control *Pacsin2*$^{+/+}$ MKs, reminiscent of MKs lacking FlnA [25]. *Pacsin2* deletion in mice recapitulates genomic studies in humans where *PACSIN2* SNPs have been associated with platelet parameters [9–14]. Since most *PACSIN2* SNPs are substitutions in intronic regions, we speculate that these variants affect how *PACSIN2* mRNA interacts with other biomolecules, thereby regulating its half-life and/or ribosome recruitment and, ultimately, the amount of PACSIN2 protein expressed in MKs. How *PACSIN2* SNPs affect MK maturation and/or platelet production remains to be determined.

PACSIN2 deletion led to bleeding diathesis due to severe thrombus embolization in vivo. The phenotype was intrinsic to platelets, as injection of *Pacsin2*$^{+/+}$ platelets into *Pacsin2*$^{-/-}$ mice normalized thrombus formation in vivo. *Pacsin2* deletion accelerated the clotting time, rendering thrombi more fragile and unstable, thereby leading to increased bleeding. Integrin β1 was hyperactive, based on increased spreading of *Pacsin2*$^{-/-}$ platelets onto surfaces coated with the integrin α2β1-specific GFOGER peptide and increased binding of the anti-active integrin β1 antibody 9EG7 to resting *Pacsin2*$^{-/-}$ platelets. Genetic deletion of platelet integrin β1 using the transgenic *Pf4-Cre* mouse normalized the mild thrombocytopenia, increased PDW, bleeding diathesis, and clotting time of *Pacsin2*$^{-/-}$ mice, but not the decreased MCV and MCH, and other blood parameters were comparable to controls. The data confirmed that the bleeding phenotype of *Pacsin2*$^{-/-}$ mice was specific and intrinsic to hyperactive platelet integrin β1. The notion was further corroborated by normal *Pacsin2*$^{-/-}$ platelet hemostatic functions when stimulated via GPVI or by thrombin, including α-granule secretion, integrin αIIbβ3 activation, aggregation, spreading onto fibrinogen, and clot retraction.

Previous studies have shown that platelet integrin β1 is dispensable to hemostasis [28, 41–43]. Increasing evidence shows that integrin hyperactivation leads to thrombocytopenia and hemostatic function defects. Gain-of-function mutations in integrin αIIb and β3 subunits have been associated with macrothrombocytopenia in patients with Glanzmann thrombasthenia [44–48]. Lack of glycan maturation on integrin β1 also leads to integrin β1 hyperactivation and consequent severe thrombocytopenia and bleeding in *B4galt1*$^{Plt-/-}$ mice [28]. Our data support the notion that integrin β1 hyperactivation, rather than deletion, led to thrombocytopenia and hemostatic function defects in *Pacsin2*$^{-/-}$ mice. Thus, control of integrin β1 function is crucial for platelet function and hemostasis.

How does PACSIN2 deletion lead to platelet integrin β1 hyperactivity? We have previously shown that the tip of the PACSIN2 F-BAR domain binds to FlnA repeat 20, thereby regulating membrane tubulation in platelets and in MKs [25]. FlnA participates in the anchoring of platelet receptors, notably GPIbα and integrin β-subunits, to the actin cytoskeleton [16]. PACSIN2 over-expression in Xenopus XTC cells prevents the localization of integrin α5β1 to focal adhesions and FlnA to stress fibers [24]. The interaction between FlnA and integrin β-subunits requires FlnA repeat 21 and a region in the cytoplasmic tail of integrin β-subunits, which overlaps with the binding sites for talin and kindlins, required for integrin activation [19, 20]. One model proposes that FlnA competes with talin and kindlins for integrin β-subunit binding, thereby maintaining integrins in an inactive state. Ablation or decreased expression of FlnA enhances integrin-mediated cell-substrate adhesion in multiple different cell lines [49], while strengthened FlnA-integrin interaction inhibits integrin-ligand interaction and cell migration [50], showing that FlnA controls integrin β1 activation. In full-length FlnA, repeats 16-21 form a compact “propeller-like” structure, in which repeats 16-17, 18-19, and 20-21 are paired [51, 52]. Importantly, repeat 21 pairs with incompletely folded repeat 20, a β-strand of which masks the integrin binding site on repeat 21 (Figure 4G, **top panel)** [22, 23]. Our biochemical data showed that a PACSIN2 peptide mimicking the FlnA repeat 20 binding site mediated binding of FlnA repeats 16-23 to integrin β7, a model for integrin β-subunits [19], suggesting that PACSIN2 binding to FlnA repeat 20

induces conformational changes in repeats 20-21, thereby unmasking the integrin binding site in repeat 21.

Why does PACSIN2 deletion affect integrin β1, but not integrin β3? Platelets contain about 80,000 αIIbβ3 molecules, compared to about 5000 α2β1 and 2000 α5β1, within the range of PACSIN2 [25]. Perhaps there is insufficient PACSIN2 molecules in platelets to affect the abundantly expressed integrin αIIbβ3 measurably. Differences in integrin β1 and β3 cytoplasmic tails provide another possibility. Proteins binding to FlnA contain a FlnA-binding motif composed of nine amino acids, in which alternate residues at odd positions are nonpolar or neutral and residue at position 3 is a conserved serine (Figure 4G, **bottom panel)** [16]. In membrane receptors, such as GPIbα and integrins β7 and β2 [18–20], the FlnA-binding motif is flanked by prolines, which in integrins are parts of tandem endocytic NPxY/F motifs and docking sites for talin and kindlins. While integrin β1 has an optimal FlnA-binding motif, integrin β3 contains an acidic glutamate at position 3, instead of a neutral serine, and lacks a C-terminal flanking proline. Thus, integrin β3 is expected to be a weaker ligand for FlnA, compared to β1. Consistently, basal integrin αIIbβ3 activation has not been observed in mouse platelets lacking FlnA or in human and mouse platelets expressing a FlnA gain-of-function mutant [34, 53, 54]. However, based on structural studies, a model has been proposed whereby FlnA repeat 21 clasps together the αIIb and β3 cytoplasmic tails, thereby preventing spontaneous αIIbβ3 activation [55]. FlnA associates with both inactive and talin-bound active αIIbβ3 to mediate platelet spreading, suggesting that the αIIb-FlnA-actin linkage promotes αIIbβ3 outside-in signaling [56]. Whether integrin β1 is hyperactive in *Flna*$^{Plt-/-}$ platelets awaits investigation.

One limitation of our study is the lack of understanding of which integrin β1 ligand plays a critical role in causing hemostatic defects in *Pacsin2*$^{-/-}$ mice. Platelets contain integrins α2β1, α5β1, and α6ββ1, which mediate adhesion to the extracellular matrix proteins collagen, fibronectin, and laminin, respectively. Fibronectin has a soluble form, called plasma fibronectin, which incorporates into blood clots, where it also binds αIIbβ3 [57]. Integrin α5β1 is a functionally critical receptor for efficient platelet adhesion, activation, and aggregation [58]. In the absence of α5β1, αIIbβ3 is inefficient in promoting normal platelet adhesion, activation, and aggregation, emphasizing the non-redundant function of α5β1 in these processes.

5. Conclusion

In conclusion, our study shows that *Pacsin2*$^{-/-}$ mice develop mild thrombocytopenia with increased PDW and slightly enlarged platelets, consistent with genomic studies. *Pacsin2*$^{-/-}$ mice also display bleeding diathesis due to platelet integrin β1 hyperactivation leading to severe thrombus embolization. In vitro, PACSIN2 mediates the binding of integrin β-subunits to FlnA. Our future studies will explore the molecular mechanisms by which PACSIN2 binding to FlnA prevents spontaneous integrin β1 activation, with a focus on how plasma fibronectin binding to platelet α5β1 contributes to the hemostatic function defects of *Pacsin2*$^{-/-}$ mice.

Supplementary Material

Refer to Web version on PubMed Central for supplementary material.

Acknowledgements

We thank Terese Jönsson Yudovich, Hilary Christensen, and Grace Kelly for technical assistance, Jon Wieser for image analysis, and Drs. Robert Flaumenhaft and Wolfgang Bergmeier for helpful discussion.

Funding

This work was supported by National Institutes of Health, National Heart, Lung, and Blood Institute grants HL102035 (QS), HL089224, HL141954, HL151333 (KMH), and HL126743 (HF). WHAK is supported by Canadian Institutes of Health Research grant PJT-183662.

References

1. Broos K, Feys HB, De Meyer SF, Vanhoorelbeke K, Deckmyn H. Platelets at work in primary hemostasis. Blood reviews. 2011; 25: 155–67. [PubMed: 21496978]
2. Ruggeri ZM. Mechanisms initiating platelet thrombus formation. Thrombosis and haemostasis. 1997; 78: 611–6. [PubMed: 9198225]
3. Bennett JS. Structure and function of the platelet integrin alphaIIbbeta3. The Journal of clinical investigation. 2005; 115: 3363–9. [PubMed: 16322781]
4. Nuyttens BP, Thijs T, Deckmyn H, Broos K. Platelet adhesion to collagen. Thrombosis research. 2011; 127 Suppl 2: S26–9.
5. Salzer U, Kostan J, Djinovic-Carugo K. Deciphering the BAR code of membrane modulators. Cellular and molecular life sciences : CMLS. 2017; 74: 2413–38. [PubMed: 28243699]
6. Rowley JW, Oler AJ, Tolley ND, et al. Genome-wide RNA-seq analysis of human and mouse platelet transcriptomes. Blood. 2011; 118: e101–11. [PubMed: 21596849]
7. Burkhart JM, Vaudel M, Gambaryan S, et al. The first comprehensive and quantitative analysis of human platelet protein composition allows the comparative analysis of structural and functional pathways. Blood. 2012; 120: e73–82. [PubMed: 22869793]
8. Zeiler M, Moser M, Mann M. Copy number analysis of the murine platelet proteome spanning the complete abundance range. Molecular & cellular proteomics : MCP. 2014; 13: 3435–45. [PubMed: 25205226]
9. Eicher JD, Chami N, Kacprowski T, et al. Platelet-Related Variants Identified by Exomechip Meta-analysis in 157,293 Individuals. American journal of human genetics. 2016; 99: 40–55. [PubMed: 27346686]
10. Astle WJ, Elding H, Jiang T, et al. The Allelic Landscape of Human Blood Cell Trait Variation and Links to Common Complex Disease. Cell. 2016; 167: 1415–29 e19. [PubMed: 27863252]
11. Chen MH, Raffield LM, Mousas A, et al. Trans-ethnic and Ancestry-Specific Blood-Cell Genetics in 746,667 Individuals from 5 Global Populations. Cell. 2020; 182: 1198–213 e14. [PubMed: 32888493]
12. Vuckovic D, Bao EL, Akbari P, et al. The Polygenic and Monogenic Basis of Blood Traits and Diseases. Cell. 2020; 182: 1214–31 e11. [PubMed: 32888494]
13. Kachuri L, Jeon S, DeWan AT, et al. Genetic determinants of blood-cell traits influence susceptibility to childhood acute lymphoblastic leukemia. American journal of human genetics. 2021; 108: 1823–35. [PubMed: 34469753]
14. GWAS Catalog, Gene: PACSIN2, https://www.ebi.ac.uk/gwas/genes/PACSIN2 [accessed 12 June 2023].
15. Risch N, Merikangas K. The future of genetic studies of complex human diseases. Science. 1996; 273: 1516–7. [PubMed: 8801636]
16. Falet H. New insights into the versatile roles of platelet FlnA. Platelets. 2013; 24: 1–5. [PubMed: 22372530]

17. Nakamura F, Osborn TM, Hartemink CA, Hartwig JH, Stossel TP. Structural basis of filamin A functions. The Journal of cell biology. 2007; 179: 1011–25. [PubMed: 18056414]
18. Nakamura F, Pudas R, Heikkinen O, et al. The structure of the GPIb-filamin A complex. Blood. 2006; 107: 1925–32. [PubMed: 16293600]
19. Kiema T, Lad Y, Jiang P, et al. The molecular basis of filamin binding to integrins and competition with talin. Molecular cell. 2006; 21: 337–47. [PubMed: 16455489]
20. Takala H, Nurminen E, Nurmi SM, et al. Beta2 integrin phosphorylation on Thr758 acts as a molecular switch to regulate 14-3-3 and filamin binding. Blood. 2008; 112: 1853–62. [PubMed: 18550856]
21. Lentaigne C, Freson K, Laffan MA, et al. Inherited platelet disorders: toward DNA-based diagnosis. Blood. 2016; 127: 2814–23. [PubMed: 27095789]
22. Lad Y, Kiema T, Jiang P, et al. Structure of three tandem filamin domains reveals auto-inhibition of ligand binding. The EMBO journal. 2007; 26: 3993–4004. [PubMed: 17690686]
23. Heikkinen OK, Ruskamo S, Konarev PV, et al. Atomic structures of two novel immunoglobulin-like domain pairs in the actin cross-linking protein filamin. The Journal of biological chemistry. 2009; 284: 25450–8. [PubMed: 19622754]
24. Cousin H, Desimone DW, Alfandari D. PACSIN2 regulates cell adhesion during gastrulation in Xenopus laevis. Developmental biology. 2008; 319: 86–99. [PubMed: 18495106]
25. Begonja AJ, Pluthero FG, Suphamungmee W, et al. FlnA binding to PACSIN2 F-BAR domain regulates membrane tubulation in megakaryocytes and platelets. Blood. 2015; 126: 80–8. [PubMed: 25838348]
26. Semmler J, Kormann J, Srinivasan SP, et al. Pacsin 2 is required for the maintenance of a normal cardiac function in the developing mouse heart. Pharmacological research. 2018; 128: 200–10. [PubMed: 29107716]
27. Malinova TS, Angulo-Urarte A, Nuchel J, et al. A junctional PACSIN2/EHD4/MICAL-L1 complex coordinates VE-cadherin trafficking for endothelial migration and angiogenesis. Nature communications. 2021; 12: 2610.
28. Giannini S, Lee-Sundlov MM, Rivadeneyra L, et al. beta4GALT1 controls beta1 integrin function to govern thrombopoiesis and hematopoietic stem cell homeostasis. Nature communications. 2020; 11: 356.
29. Eaton N, Drew C, Wieser J, Munday AD, Falet H. Dynamin 2 is required for GPVI signaling and platelet hemostatic function in mice. Haematologica. 2020; 105: 1414–23. [PubMed: 31296575]
30. Eaton N, Subramaniam S, Schulte ML, et al. Bleeding diathesis in mice lacking JAK2 in platelets. Blood Adv. 2021; 5: 2969–81. [PubMed: 34342643]
31. Knight CG, Morton LF, Peachey AR, Tuckwell DS, Farndale RW, Barnes MJ. The collagen-binding A-domains of integrins alpha(1)beta(1) and alpha(2)beta(1) recognize the same specific amino acid sequence, GFOGER, in native (triple-helical) collagens. The Journal of biological chemistry. 2000; 275: 35–40. [PubMed: 10617582]
32. Emsley J, Knight CG, Farndale RW, Barnes MJ, Liddington RC. Structural basis of collagen recognition by integrin alpha2beta1. Cell. 2000; 101: 47–56. [PubMed: 10778855]
33. Morton LF, Hargreaves PG, Farndale RW, Young RD, Barnes MJ. Integrin alpha 2 beta 1-independent activation of platelets by simple collagen-like peptides: collagen tertiary (triple-helical) and quaternary (polymeric) structures are sufficient alone for alpha 2 beta 1-independent platelet reactivity. The Biochemical journal. 1995; 306 (Pt 2): 337–44. [PubMed: 7534064]
34. Falet H, Pollitt AY, Begonja AJ, et al. A novel interaction between FlnA and Syk regulates platelet ITAM-mediated receptor signaling and function. The Journal of experimental medicine. 2010; 207: 1967–79. [PubMed: 20713593]
35. Lenter M, Uhlig H, Hamann A, Jeno P, Imhof B, Vestweber D. A monoclonal antibody against an activation epitope on mouse integrin chain beta 1 blocks adhesion of lymphocytes to the endothelial integrin alpha 6 beta 1. Proceedings of the National Academy of Sciences of the United States of America. 1993; 90: 9051–5. [PubMed: 7692444]
36. Bazzoni G, Shih DT, Buck CA, Hemler ME. Monoclonal antibody 9EG7 defines a novel beta 1 integrin epitope induced by soluble ligand and manganese, but inhibited by calcium. The Journal of biological chemistry. 1995; 270: 25570–7. [PubMed: 7592728]

37. Schroeder JA, Kuether EA, Fang J, et al. Thromboelastometry assessment of hemostatic properties in various murine models with coagulopathy and the effect of factor VIII therapeutics. Journal of thrombosis and haemostasis : JTH. 2021; 19: 2417–27. [PubMed: 34245090]
38. Stefanini L, Lee RH, Paul DS, et al. Functional redundancy between RAP1 isoforms in murine platelet production and function. Blood. 2018; 132: 1951–62. [PubMed: 30131434]
39. Ehrlicher AJ, Nakamura F, Hartwig JH, Weitz DA, Stossel TP. Mechanical strain in actin networks regulates FilGAP and integrin binding to filamin A. Nature. 2011; 478: 260–3. [PubMed: 21926999]
40. Durrant TN, van den Bosch MT, Hers I. Integrin alphaIIbbeta3 outside-in signaling. Blood. 2017; 130: 1607–19. [PubMed: 28794070]
41. Nieswandt B, Brakebusch C, Bergmeier W, et al. Glycoprotein VI but not alpha2beta1 integrin is essential for platelet interaction with collagen. The EMBO journal. 2001; 20: 2120–30. [PubMed: 11331578]
42. Gruner S, Prostredna M, Schulte V, et al. Multiple integrin-ligand interactions synergize in shear-resistant platelet adhesion at sites of arterial injury in vivo. Blood. 2003; 102: 4021–7. [PubMed: 12893753]
43. Petzold T, Ruppert R, Pandey D, et al. beta1 integrin-mediated signals are required for platelet granule secretion and hemostasis in mouse. Blood. 2013; 122: 2723–31. [PubMed: 24004668]
44. Kunishima S, Kashiwagi H, Otsu M, et al. Heterozygous ITGA2B R995W mutation inducing constitutive activation of the alphaIIbbeta3 receptor affects proplatelet formation and causes congenital macrothrombocytopenia. Blood. 2011; 117: 5479–84. [PubMed: 21454453]
45. Bury L, Malara A, Gresele P, Balduini A. Outside-in signalling generated by a constitutively activated integrin alphaIIbbeta3 impairs proplatelet formation in human megakaryocytes. PloS one. 2012; 7: e34449. [PubMed: 22539947]
46. Kashiwagi H, Kunishima S, Kiyomizu K, et al. Demonstration of novel gain-of-function mutations of alphaIIbbeta3: association with macrothrombocytopenia and glanzmann thrombasthenia-like phenotype. Mol Genet Genomic Med. 2013; 1: 77–86. [PubMed: 24498605]
47. Favier M, Bordet JC, Favier R, et al. Mutations of the integrin alphaIIb/beta3 intracytoplasmic salt bridge cause macrothrombocytopenia and enlarged platelet alphα-granules. Am J Hematol. 2018; 93: 195–204. [PubMed: 29090484]
48. Bury L, Zetterberg E, Leinoe EB, et al. A novel variant Glanzmann thrombasthenia due to co-inheritance of a loss- and a gain-of-function mutation of ITGB3: evidence of a dominant effect of gain-of-function mutations. Haematologica. 2018; 103: e259–e63. [PubMed: 29439184]
49. Xu Y, Bismar TA, Su J, et al. Filamin A regulates focal adhesion disassembly and suppresses breast cancer cell migration and invasion. The Journal of experimental medicine. 2010; 207: 2421–37. [PubMed: 20937704]
50. Calderwood DA, Huttenlocher A, Kiosses WB, et al. Increased filamin binding to beta-integrin cytoplasmic domains inhibits cell migration. Nature cell biology. 2001; 3: 1060–8. [PubMed: 11781567]
51. Tossavainen H, Koskela O, Jiang P, et al. Model of a six immunoglobulin-like domain fragment of filamin A (16-21) built using residual dipolar couplings. J Am Chem Soc. 2012; 134: 6660–72. [PubMed: 22452512]
52. Ruskamo S, Gilbert R, Hofmann G, et al. The C-terminal rod 2 fragment of filamin A forms a compact structure that can be extended. The Biochemical journal. 2012; 446: 261–9. [PubMed: 22676060]
53. Berrou E, Adam F, Lebret M, et al. Gain-of-Function Mutation in Filamin A Potentiates Platelet Integrin alphaIIbbeta3 Activation. Arteriosclerosis, thrombosis, and vascular biology. 2017; 37: 1087–97. [PubMed: 28428218]
54. Adam F, Kauskot A, Lamrani L, et al. A gain-of-function filamin A mutation in mouse platelets induces thrombus instability. Journal of thrombosis and haemostasis : JTH. 2022; 20: 2666–78. [PubMed: 36006037]
55. Liu J, Das M, Yang J, et al. Structural mechanism of integrin inactivation by filamin. Nat Struct Mol Biol. 2015; 22: 383–9. [PubMed: 25849143]

56. Liu J, Lu F, Ithychanda SS, et al. A mechanism of platelet integrin alphaIIbbeta3 outside-in signaling through a novel integrin alphaIIb subunit-filamin-actin linkage. Blood. 2023; 141: 2629–41. [PubMed: 36867840]

57. Wang Y, Reheman A, Spring CM, et al. Plasma fibronectin supports hemostasis and regulates thrombosis. The Journal of clinical investigation. 2014; 124: 4281–93. [PubMed: 25180602]

58. Janus-Bell E, Yakusheva A, Scandola C, et al. Characterization of the Role of Integrin alpha5beta1 in Platelet Function, Hemostasis, and Experimental Thrombosis. Thrombosis and haemostasis. 2021; 122: 767–76. [PubMed: 34598304]

Essentials

- Human genomic studies have associated variants in the F-BAR protein PACSIN2 with platelet parameters.
- Here we investigated the role of PACSIN2 in platelet function.
- Mice lacking PACSIN2 develop mild thrombocytopenia and prolonged bleeding time due to severe thrombus embolization in vivo.
- PACSIN2 negatively regulates platelet integrin β1 hemostatic function.

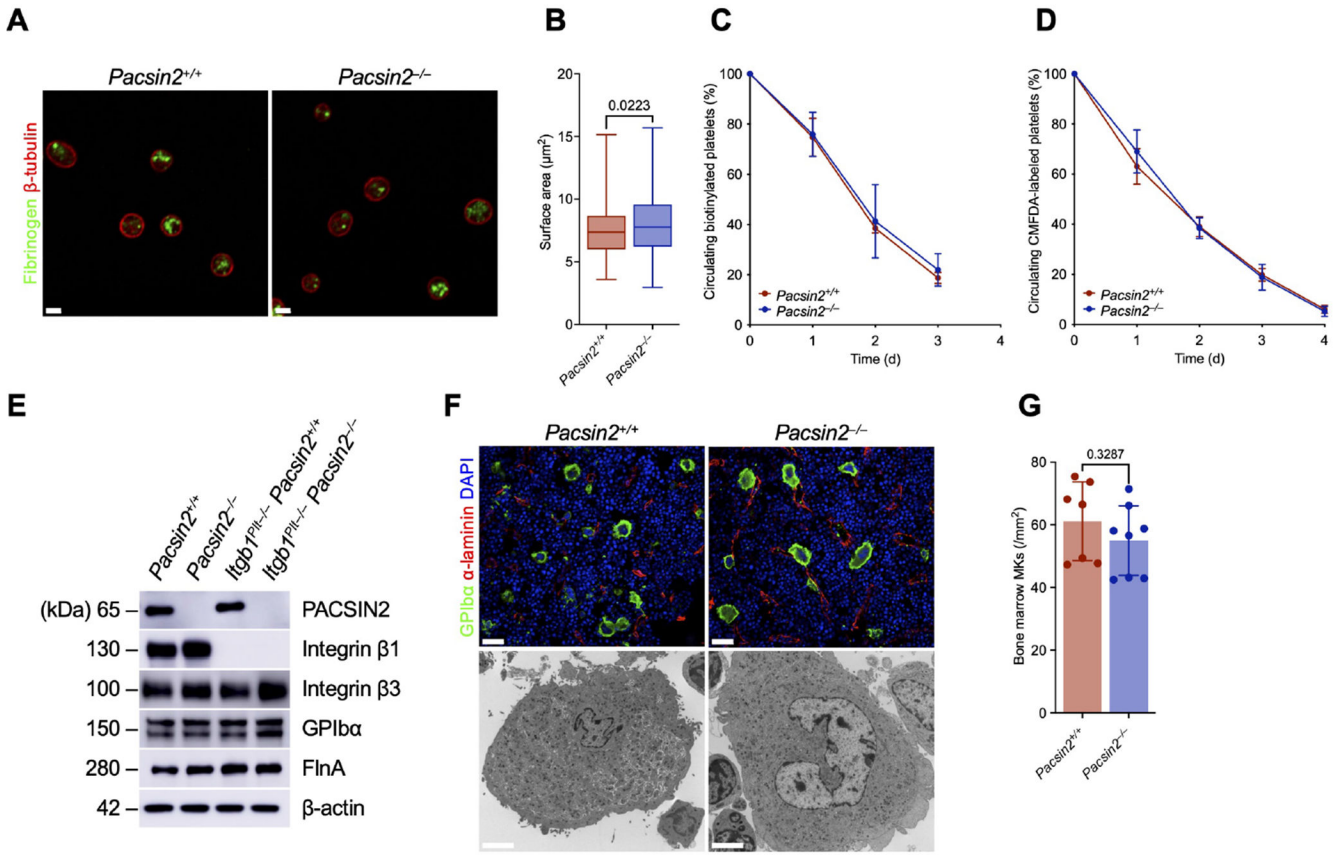

Figure 1. Characterization of *Pacsin2*$^{-/-}$ platelets and megakaryocytes.

(A) Immunofluorescence analysis of fibrinogen (green) and β-tubulin (red) in *Pacsin2*$^{+/+}$ and *Pacsin2*$^{-/-}$ platelets on BSA. Scale bars, 2 μm. **(B)** Surface area of resting platelets. Results represent mean ± SD of 239 *Pacsin2*$^{+/+}$ and 122 *Pacsin2*$^{-/-}$ and were compared by using the unpaired Student t test ($P = .0223$). **(C)** Biotin NHS was injected into *Pacsin2*$^{+/+}$ and *Pacsin2*$^{-/-}$ mice and blood samples were collected at the indicated time points. **(D)** CMFDA-labeled *Pacsin2*$^{+/+}$ and *Pacsin2*$^{-/-}$ platelets were injected into *Pacsin2*$^{+/+}$ mice and blood samples were collected at the indicated time points. The percentage of biotin- or CMFDA-positive platelets in circulation was determined by flow cytometry, compared to <2 min post injection (100%). Results are mean ± SD of 3-5 independent experiments. **(E)** *Pacsin2*$^{+/+}$ and *Pacsin2*$^{-/-}$ platelet lysates corresponding to 2 mg of protein were subjected to SDS-PAGE and probed for the indicated proteins. Results are representative of 3 independent experiments. **(F) Top.** Seven-mm-thick femur bone marrow sections from *Pacsin2*$^{+/+}$ and *Pacsin2*$^{-/-}$ mice were immunostained for resident MKs and vasculature using anti-GPIbα (green) and anti-laminin (red) antibodies, respectively. Scale bars, 30 μm. Sections shown are representative of 7 mice per genotype. **Bottom.** Transmission electron microscopy analysis of freshly isolated bone marrow *Pacsin2*$^{+/+}$ and *Pacsin2*$^{-/-}$ MKs. Scale bars, 2 μm. **(G)** Bone marrow MK counts (n = 7 *Pacsin2*$^{+/+}$ and 8 *Pacsin2*$^{-/-}$; $P = .3287$).

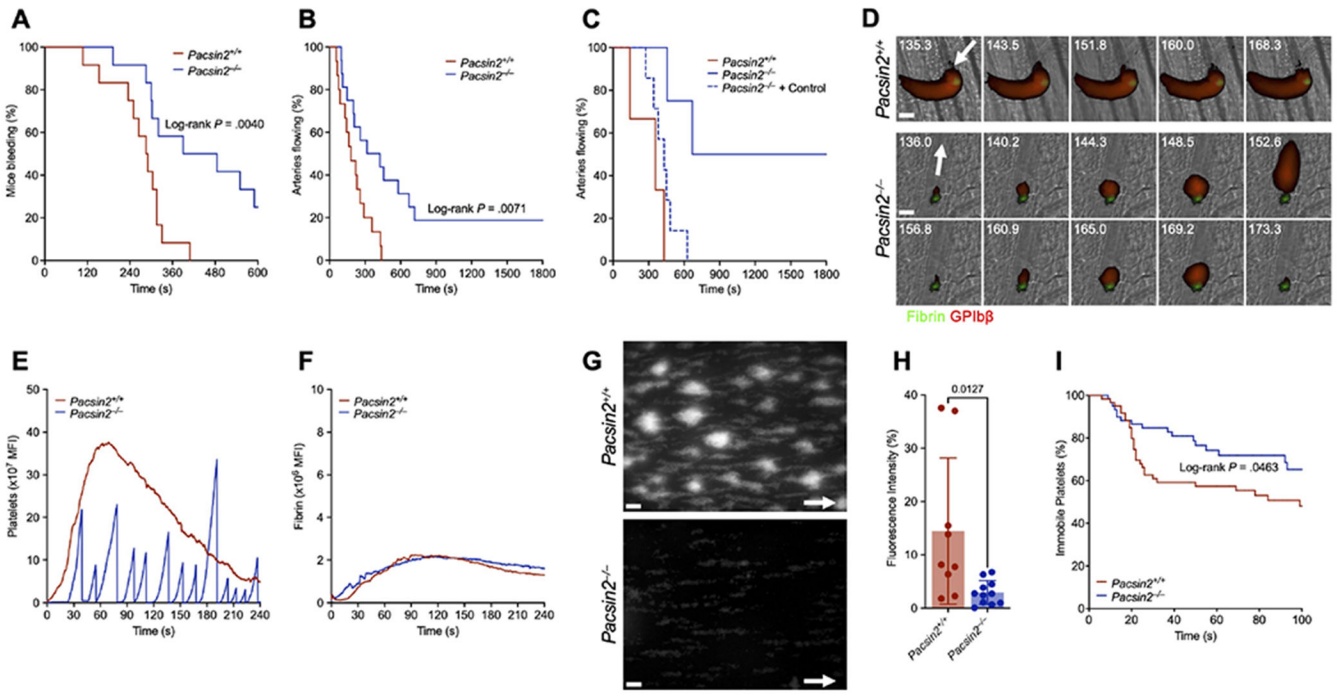

Figure 2. Increased bleeding time and thrombus formation defects in *Pacsin2*$^{-/-}$ mice.

(A) Tail-bleeding time of *Pacsin2*$^{+/+}$ and *Pacsin2*$^{-/-}$ mice (n = 12 in each group). Results were estimated by the Kaplan-Meier method and were compared by using the log-rank test (log-rank $P = .0040$). **(B)** Time to occlusion after $FeCl_3$-induced injury. *Pacsin2*$^{+/+}$ (n = 15) and *Pacsin2*$^{-/-}$ (n = 16) carotid arteries were exposed to 10% $FeCl_3$ for 3 min, and arterial flow rates were measured. Results were estimated by the Kaplan-Meier method and were compared by using the log-rank test (log-rank $P = .0071$). **(C)** Injection of 80 x 10^6 control *Pacsin2*$^{+/+}$ platelets into *Pacsin2*$^{-/-}$ mice normalized their median time to occlusive thrombosis (n = 6 in each group). *Pacsin2*$^{+/+}$ and *Pacsin2*$^{-/-}$ mice were injected with anti-GPIbβ (red) and anti-fibrin (green) antibodies, and the cremaster arteries were interrogated with a 3i Ablate! laser during fluorescence, real-time, and intravital video microscopy. **(D)** Representative still images. Arrows represent blood flow direction. Time in s. Scale bars, 20 μm. Platelet **(E)** and fibrin **(F)** accumulation at the site of injury was measured by fluorescence intensity. PPACK-anticoagulated whole blood from *Pacsin2*$^{+/+}$ and *Pacsin2*$^{-/-}$ mice was labeled and perfused on a type I collagen-immobilized surface at an arterial shear rate of 1500 s^{-1}. **(G)** Representative still images at 3 min. Bars represent 100 mm. **(H)** Fluorescence intensity at 3 minutes. Results represent mean ± SD and were compared by using the unpaired Student t test (n = 9 *Pacsin2*$^{+/+}$ and 11 *Pacsin2*$^{-/-}$; $P = .0127$). **(I)** Dwell time of individual *Pacsin2*$^{+/+}$ and *Pacsin2*$^{-/-}$ platelets. Results were estimated by the Kaplan-Meier method and were compared by using the log-rank test (n = 60 in each group; log-rank $P = .0463$).

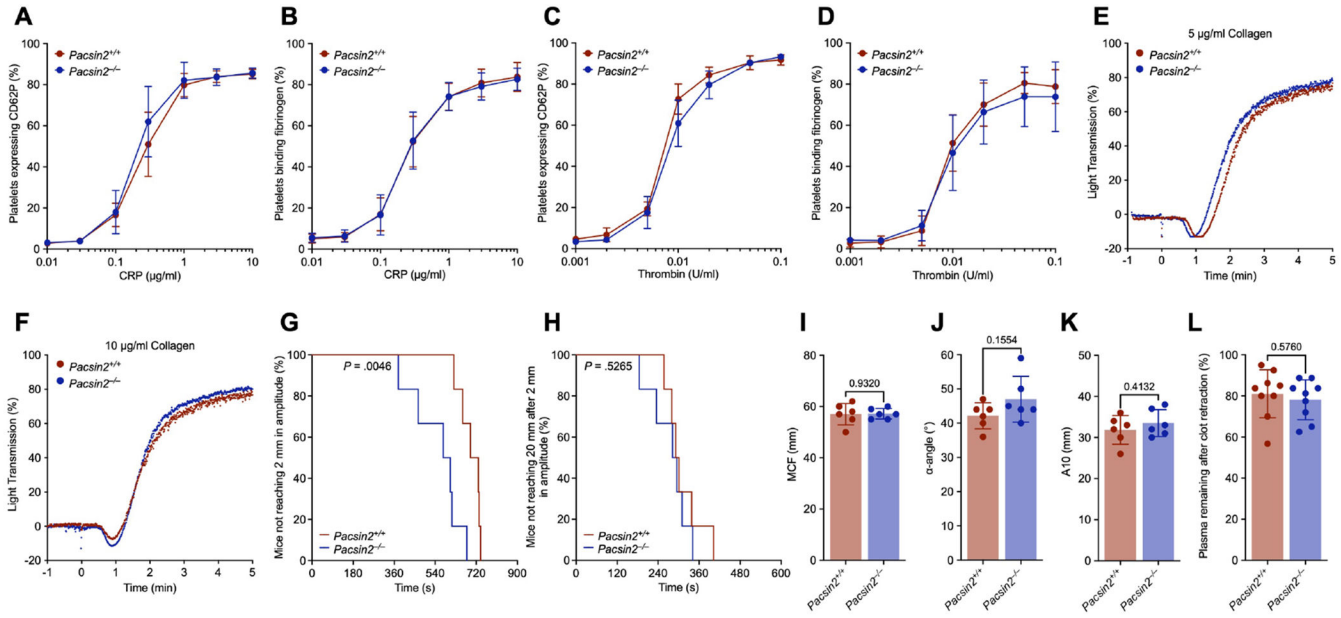

Figure 3. Hemostatic functions of *Pacsin2*$^{-/-}$ platelets.

Pacsin2$^{+/+}$ and *Pacsin2*$^{-/-}$ platelets were activated for 2 min at 37°C with CRP **(A,B)** or thrombin **(C,D)**, incubated with FITC-labeled anti-mouse CD62P antibody **(A,C)** or Oregon Green 488-labeled fibrinogen **(B,D)**, and analyzed by flow cytometry. Results are expressed as a percentage of positive platelets and represent mean ± SD of 3-6 independent experiments. Aggregation of *Pacsin2*$^{+/+}$ and *Pacsin2*$^{-/-}$ platelets was determined by light transmission under stirring conditions at 37°C in response to 5 μg/mL **(E)** or 10 μg/mL **(F)** of collagen. Graphs are representative of 4 independent experiments. *Pacsin2*$^{+/+}$ and *Pacsin2*$^{-/-}$ blood samples were analyzed using the ROTEM assay. Clotting time **(G)** and clot formation time **(H)** of *Pacsin2*$^{+/+}$ and *Pacsin2*$^{-/-}$ blood samples. Results were estimated by the Kaplan-Meier method and were compared by using the log-rank test (n = 6 in each group; log-rank P = .0046 and .5265, respectively). Maximum clot firmness (MCF) **(I),** α-angle **(J),** and A10 **(K)**. Results represent mean ± SD of 6 independent experiments. **(L)** Washed *Pacsin2*$^{+/+}$ and *Pacsin2*$^{-/-}$ platelets were added to human platelet-poor plasma in ACD containing 5 mM $CaCl_2$ and 0.2 U/mL thrombin in siliconized cuvettes (n = 9 in each group).

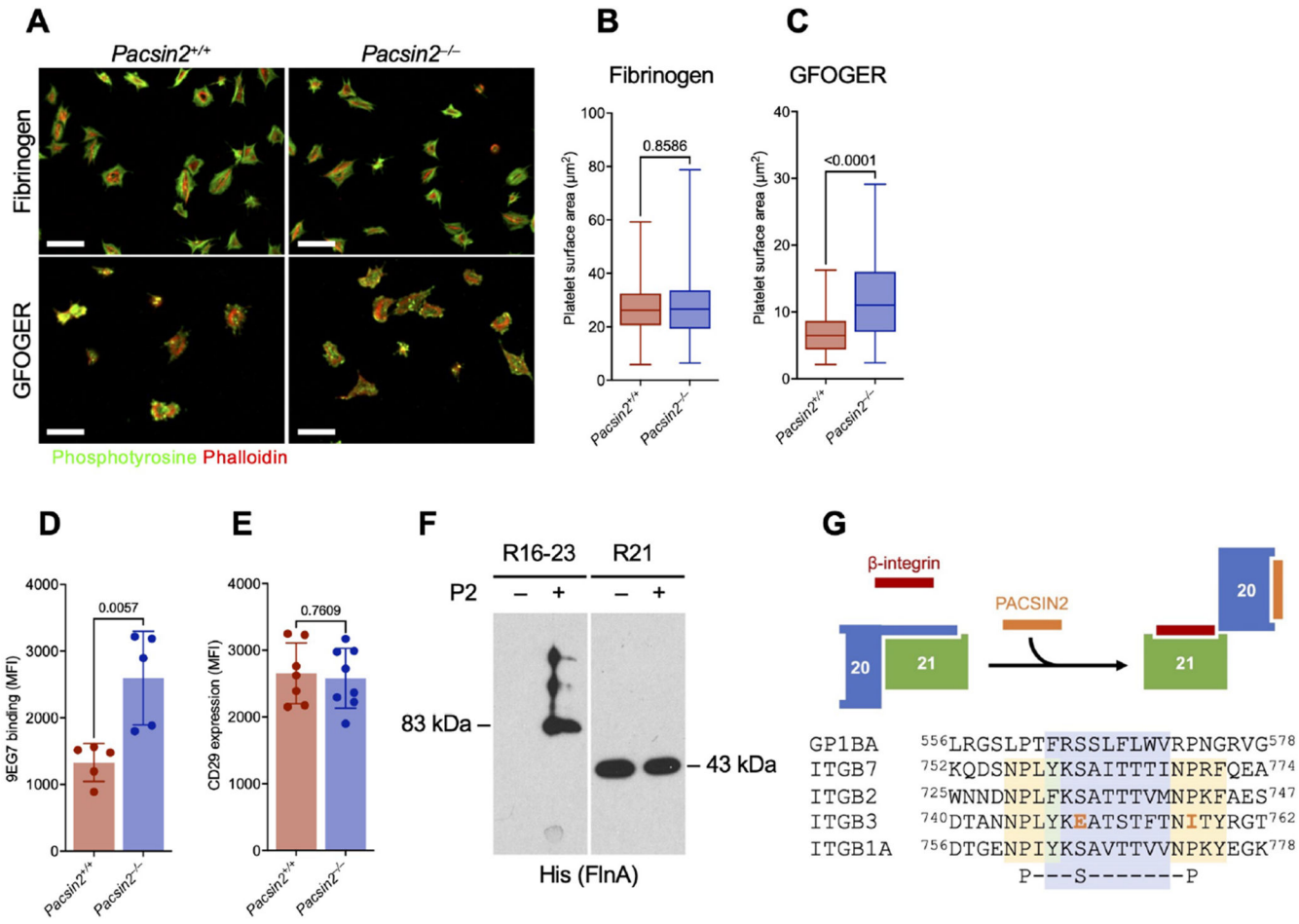

Figure 4. Hyperactive integrin β1 in *Pacsin2*$^{-/-}$ platelets.

(A) *Pacsin2*$^{+/+}$ and *Pacsin2*$^{-/-}$ platelets were activated with 1 μg/mL CRP and left to adhere to 100 μg/mL fibrinogen or 20 μg/mL GFOGER for 30 min at 37°C. Fixed platelets were stained for phosphotyrosine (4G10, green) and F-actin (phalloidin, red) and analyzed by immunofluorescence. Immunofluorescence micrographs representative of four independent experiments. Scale bars, 10 μm. **(B)** Surface area of 388 *Pacsin2*$^{+/+}$ and 635 *Pacsin2*$^{-/-}$ platelets on fibrinogen ($P = .8586$). **(C)** Surface area of 56 *Pacsin2*$^{+/+}$ and 40 *Pacsin2*$^{-/-}$ platelets on GFOGER ($P < .0001$). Results represent the mean ± SD and were compared by using the unpaired Student t-test. *Pacsin2*$^{+/+}$ and *Pacsin2*$^{-/-}$ platelets were incubated with rat anti-mouse active integrin β1 antibody 9EG7 (n = 5 in each group; $P = .0057$) **(D)** or hamster anti-mouse total integrin β1 antibody (n = 7 *Pacsin2*$^{+/+}$ and 8 *Pacsin2*$^{-/-}$; $P = .7609$) **(E)** and analyzed by flow cytometry. **(F)** An integrin β7 peptide containing the FlnA repeat 21 binding site (residues 752-770) was conjugated to SulfoLink agarose resin and incubated with His-tagged FlnA repeats 16-23 (left panel) or 21 (right panel) in the presence (+) or absence (−) of a PACSIN2 peptide (P2) mimicking the FlnA repeat 20 binding site (residues 171-189) as indicated. Complexes were subjected to SDS-PAGE and probed for His (FlnA). **(G) Top.** Hypothetic model on the role of PACSIN2 in β-integrin regulation by FlnA. In full-length FlnA, a β-strand in incompletely folded repeat 20 masks the β-integrin binding site on repeat 21. PACSIN2 binding to repeat 20 initiates major

conformational changes in FlnA, resulting in the unmasking of repeat 21 and binding of β-integrin. **Bottom.** Alignment of GPIbα and β-integrin FlnA-binding motifs (blue highlight), flanked by endocytic NPxY/F motifs in integrins (yellow highlight). Integrin β1 has an optimal FlnA-binding motif, while integrin β3 contains an acidic glutamate at position 749, instead of a neutral serine, and lacks a C-terminal flanking proline at position 757 (orange).

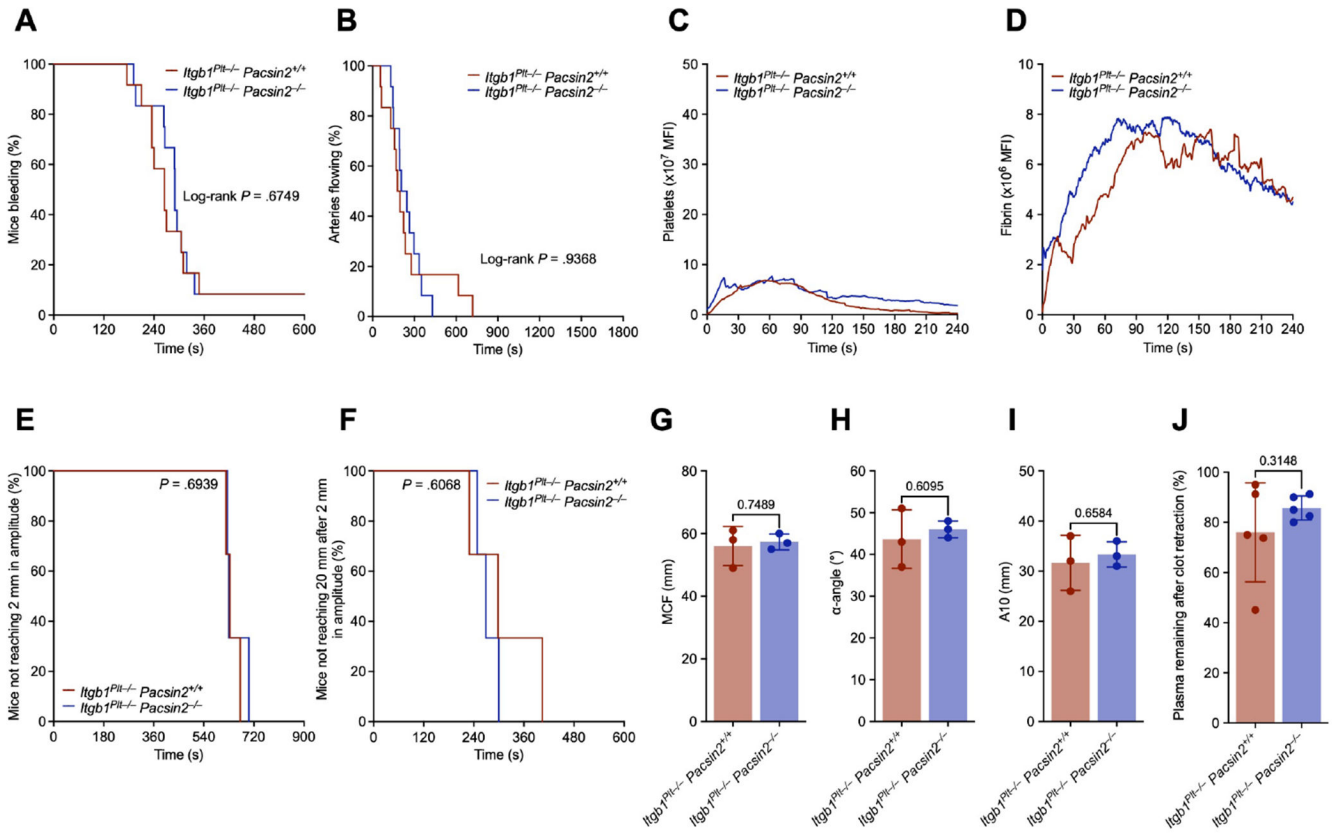

Figure 5. Platelet-specific integrin β1 deletion normalizes the thrombus formation defects of *Pacsin2*$^{-/-}$ mice.

(A) Tail-bleeding time of *Itgb1*$^{Plt-/-}$ *Pacsin2*$^{+/+}$ and *Itgb1*$^{Plt-/-}$ *Pacsin2*$^{-/-}$ mice (n = 12 in each group). Results were estimated by the Kaplan-Meier method and were compared by using the log-rank test (log-rank $P = .6749$). **(B)** Time to occlusion after $FeCl_3$-induced injury. *Itgb1*$^{Plt-/-}$ *Pacsin2*$^{+/+}$ and *Itgb1*$^{Plt-/-}$ *Pacsin2*$^{-/-}$ carotid arteries were exposed to 10% $FeCl_3$ for 3 min, and arterial flow rates were measured (n = 12 in each group). Results were estimated by the Kaplan-Meier method and were compared by using the log-rank test (n = 16 in each group; log-rank $P = .9368$). *Itgb1*$^{Plt-/-}$ *Pacsin2*$^{+/+}$ and *Itgb1*$^{Plt-/-}$ *Pacsin2*$^{-/-}$ mice were injected with anti-GPIbβ (red) and anti-fibrin (green) antibodies, and the cremaster arteries were interrogated with a 3i Ablate! laser during fluorescence, real-time, and intravital video microscopy. Platelet **(C)** and fibrin **(D)** accumulation at the site of injury was measured by fluorescence intensity. Clotting time **(E)** and clot formation time **(F)** of *Itgb1*$^{Plt-/-}$ *Pacsin2*$^{+/+}$ and *Itgb1*$^{Plt-/-}$ *Pacsin2*$^{-/-}$ blood samples using the native ROTEM assay. Results were estimated by the Kaplan-Meier method and were compared by using the log-rank test (n = 3 in each group; log-rank $P = .6939$ and .6068, respectively). Maximum clot firmness (MCF) **(G)**, α-angle **(H)**, and A10 **(I)**. Results represent mean ± SD of 3 independent experiments. **(J)** Washed *Itgb1*$^{Plt-/-}$ *Pacsin2*$^{+/+}$ and *Itgb1*$^{Plt-/-}$ *Pacsin2*$^{-/-}$ platelets were added to human platelet-poor plasma in ACD containing 5 mM $CaCl_2$ and 0.2 U/mL thrombin in siliconized cuvettes (n = 5 in each group).

Table 1.

Hematological and platelet parameters in *Pacsin2*$^{-/-}$ mice

Parameter	*Pacsin2*$^{+/+}$	*Pacsin2*$^{-/-}$	*P*-value
Platelets			
Platelets (10^3/μL)	1178 ± 135	899 ± 267	.0043
MPV (fL)	4.8 ± 0.3	4.9 ± 0.2	.3086
PDW (fL)	6.6 ± 0.2	6.9 ± 0.2	.0054
Erythrocytes			
Erythrocytes (10^3/μL)	9118 ± 1504	8571 ± 1332	.3554
MCV (fL)	44.2 ± 1.7	41.6 ± 1.2	.0004
MCH (pg)	14.4 ± 0.9	13.6 ± 0.4	.0133
MCHC (g/dL)	32.9 ± 0.6	32.7 ± 0.7	.6145
Hemoglobin (g/dL)	13.1 ± 1.9	11.7 ± 1.9	.0961
Hematocrit (%)	39.8 ± 5.7	35.8 ± 6.1	.1127
Leukocytes			
Lymphocytes (10^3/μL)	9.40 ± 3.39	10.18 ± 2.43	.5246
Granulocytes (10^3/μL)	1.34 ± 0.49	1.26 ± 0.55	.7107
Monocytes (10^3/μL)	0.72 ± 0.40	1.04 ± 0.46	.0787
Platelet surface glycoproteins			
GPIbα (CD42b)	3012 ± 722	2860 ± 4580	.6309
GPIbβ (CD42c)	914 ± 310	1177 ± 437	.2094
GPIX (CD42a)	1589 ± 304	2015 ± 564	.0983
GPV (CD42d)	722 ± 236	785 ± 196	.5771
GPVI	424 ± 120	408 ± 34	.7234
integrin β3 (CD61, GPIIIa)	1036 ± 283	1154 ± 278	.4284
integrin αIIb (CD41, GPIIb)	4418 ± 646	4584 ± 241	.5099
integrin β1 (CD29, GPIIa)	2654 ± 456	2581 ± 449	.7609
integrin α2 (CD49b, GPIa)	359 ± 81	337 ± 51	.5370
integrin α5 (CD49e, GPIc)	72 ± 23	70 ± 17	.8400

Complete blood count (n = 12 in each group). Platelet surface glycoproteins were detected by flow cytometry. Data represent mean fluorescence intensity (n = 7 *Pacsin2*$^{+/+}$ and 8 *Pacsin2*$^{-/-}$). MPV, mean platelet volume; PDW, platelet distribution width; MCV, mean corpuscular volume; MCH, mean corpuscular hemoglobin; MCHC, mean corpuscular hemoglobin concentration.

Table 2.

Hematological and platelet parameters in *Itgb1*$^{Plt-/-}$ *Pacsin2*$^{-/-}$ mice

Parameter	*Itgb1*$^{Plt-/-}$ *Pacsin2* $^{+/+}$	*Itgb1*$^{Plt-/-}$ *Pacsin2*$^{-/-}$	*P*-value
Platelets			
Platelets (10^3/μL)	1176 ± 169	1289 ± 165	.1194
MPV (fL)	5.0 ± 0.2	5.0 ± 0.2	.9942
PDW (fL)	6.7 ± 0.2	6.7 ± 0.2	.6444
Erythrocytes			
Erythrocytes (10^3/μL)	9153 ± 1078	9145 ± 623	.9835
MCV (fL)	44.7 ± 1.7	40.8 ± 1.2	<.0001
MCH (pg)	14.7 ± 0.8	13.3 ± 0.4	<.0001
MCHC (g/dL)	33.0 ± 0.9	32.7 ± 0.5	.4417
Hemoglobin (g/dL)	13.5 ± 1.6	12.7 ± 2.1	.3143
Hematocrit (%)	40.9 ± 4.4	38.8 ± 6.1	.3522
Leukocytes			
Lymphocytes (10^3/μL)	9.12 ± 2.73	11.55 ± 3.26	.0565
Granulocytes (10^3/μL)	1.30 ± 0.33	1.15 ± 0.39	.2685
Monocytes (10^3/μL)	0.62 ± 0.40	0.68 ± 0.37	.6731
Platelet surface glycoproteins			
GPIbα (CD42b)	3092 ± 1061	3473 ± 602	.5052
GPIbβ (CD42c)	797 ± 286	1105 ± 314	.1732
GPIX (CD42a)	2047 ± 824	2288 ± 592	.6101
GPV (CD42d)	927 ± 238	981 ± 115	.6551
GPVI	689 ± 163	541 ± 92	.1147
integrin β3 (CD61, GPIIIa)	1106 ± 267	922 ± 303	.3392
integrin αIIb (CD41, GPIIb)	5492 ± 1535	5341 ± 2125	.9007
integrin β1 (CD29, GPIIa)	17 ±5	13 ±5	.2555
integrin α2 (CD49b, GPIa)	4 ± 1	4 ± 1	.8543
integrin α5 (CD49e, GPIc)	1 ± 1	1 ± 1	.7736

Complete blood count (n = 12 in each group). Platelet surface glycoproteins were detected by flow cytometry. Data represent mean fluorescence intensity (n = 5 in each group).